Piecewise Gamma Corrected Optimally Framed Grumwald-Letnikov Fractional Differential Masking for Satellite Image Enhancement

Himanshu Singh, Anil Kumar, L. K. Balyan and H. N. Lee

***Abstract*—In this paper, a highly efficient biologically inspired Lévy-flight firefly algorithm based optimally weighted piecewise-gamma-corrected Grumwald-Letnikov (GL) fractional differential (FD) masking is presented for quality enhancement of densely textured, remotely sensed dark satellite images. The key intelligence is to utilize a weighted summation of intensity as well as texture based enhancement along with an efficiently defined cost function. The cost function is framed such that, more and more intensity span can be explored in a positive manner. Here, an efficient fractional order differentiation based unsharp masking, takes care for enhancing the texture content of the images along with desired restoration of all kinds of local edges. In association with it, piecewise gamma correction is also imparted to enhance the intensity channel of the input image. Rigorous experimentation is executed by employing the performance evaluation and comparison with pre-existing recently proposed and highly appreciated quality enhancement approaches.**

***Index Terms*—Fractional-order masking; piecewise gamma correction; image quality enhancment; Grumwald-Letnikov (GL) fractional order differentiation; Lévy-flight firefly optimization.**

I. Introduction

Satellite images are usually acquired in unavoidable, unfavorable and poorly illuminated situations, in general, and hence usually requires a rigorous, efficient and highly adaptive pre-processing for intrinsic and visual quality enhancement [1]. The explicit significance of remotely acquired image is quite understood irrespective of the domain of application as most of the technological human welfare advancements rely on it [2]. Wide variety of methodologies are already available in literature for general images as discussed in [1-2]. Initially, general histogram equalization (GHE) [3] was introduced, and then, its multiple variants have been proposed. In the same context, necessity of localized processing seems more aspiring and hence various sub-equalization inspired histogram based enhancement approaches have been also proposed. A detailed literature analysis in this context is also available in [1-2] and out of those significant contributions some well admired state-of-the-art methods like, brightness preserved fuzzy dynamic HE [4], median-mean based sub-image clipped HE (MMSICHE) [5], recursively separated-ESIHE (RS-ESIHE) [6], averaging histogram equalization (AVHEQ) [7]; HE based optimal profile compression (HEOPC) [8], HE with maximum intensity coverage (HEMIC) [9], RHE-DCT [10], adaptive gamma correction with weighting distribution (AGCWD) [11] and its efficient variations [12-16] followed by the intensity and edge based adaptive unsharp masking filter (IEUMF) [17] based enhancement are studied here and re-implemented for desired performance evaluation and comparison with the proposed Piecewise-Gamma-Corrected Optimally Framed Grumwald-Letnikov FD Masking [18] for Image Enhancement. Rest of the paper is drafted as: Section II deals with the proposed FD mask framing strategy and the proposed methodology. Performance evaluation and comparison based Experimental results are presented in Section III and finally, conclusions are drawn in Section IV.

Himanshu Singh, Anil Kumar and L. K. Balyan are with Indian Institute of Information Technology Design and Manufacturing, Jabalpur, India (e-mail: himanshu.iiitj@ieee.org; {anilkdee; lokendra.balyan}@gmail.com).

H. N. Lee is with Gwangju Institute of Science and Technology, Gwangju, South Korea. (e-mail: heungno@gist.ac.kr).

II. Proposed Methodology

Parallel band processing is generally required for multiband images, but for enhancing equivalent color images, Hue-Saturation-Intensity (HSI) model can be applied to decouple the chromatic as well as non-chromatic information, as [3]:

$$\left[H(m,n),S(m,n),I(m,n)\right]^T = T_{RGB}^{HSI}\left[R(m,n),G(m,n),B(m,n)\right]^T, \quad (1)$$

Here, T_{RGB}^{HSI} is *RGB* to *HSI* transformation process. The color image enhancement can be done through processing only the luminance intensity channel, along with preserving hue and saturation channels' content as such, followed by linear stretching. The gamma compressed interim intensity channel can be evaluated as [1]:

$$I_{gcp} = \left(I_{in}\right)^{\gamma}, \qquad \gamma > 1, \quad (2)$$

The corresponding gamma expanded interim intensity channel can be evaluated as [1]:

$$I_{gex} = \left(I_{in}\right)^{1/\gamma}, \qquad \gamma > 1, \quad (3)$$

The FD masking filter based sharpened interim intensity channel can be evaluated as [2]:

$$I_{fdmf} = I_{in} + \eta.\xi.I_{fd}, \quad (4)$$

Here, I_{fd} mainly comprises of edges, obtained by convolutional filtering with mask (H) as follows [1]:

$$I_{fd} = I_{in} \otimes H, \quad (5)$$

Following the standard and well-appreciated $\nu -$ ordered Grumwald-Letnikov definition for FD $(\nu > 0)$ as [18]:

978-1-5386-3520-9/18/$31.00 ©2018 IEEE

$$D_{G-L}^{v} f(t) = \lim_{h \to 0} h^{-v} \sum_{k=0}^{[(t-a)/h]} (-1)^k \frac{\Gamma(v+1)}{k!\Gamma(v-k+1)} f(t-kh), \qquad (6)$$

Here, $[.]$ stands for integer portion, the span of the signal $f(t)$ is $[a,t]$, for any fraction or real number α. Here, h must be unity, as minimum in-between adjacent pixel distance is unity. The above definition when applied over a 2-D digital image, then the corresponding partial differential equation w.r.t. x and y respectively, can be framed as [18]:

$$\begin{aligned} D_x^v f(x,y) = \frac{\partial^v f(x,y)}{\partial x^v} &\approx f(x,y) + (-v) f(x-1,y) + \frac{(-v)(-v+1)}{2} f(x-2,y) \\ &+ \frac{(-v)(-v+1)(-v+2)}{6} f(x-3,y) + \ldots + \frac{\Gamma(-v+1)}{k!\,\Gamma(-v-k+1)} f(x-k,y), \end{aligned} \qquad (7)$$

$$\begin{aligned} D_y^v f(x,y) = \frac{\partial^v f(x,y)}{\partial y^v} &\approx f(x,y) + (-v) f(x,y-1) + \frac{(-v)(-v+1)}{2} f(x,y-2) \\ &+ \frac{(-v)(-v+1)(-v+2)}{6} f(x,y-3) + \ldots + \frac{\Gamma(-v+1)}{k!\,\Gamma(-v-k+1)} f(x,y-n), \end{aligned} \qquad (8)$$

To employ 2-D convolutional filtering using a 2-D FD order 5×5 *or* 7×7 masking filter, whose coefficients are derived by the proposed uniformly balanced gradient behavior along all eight directions.

$$[C_1, C_2, C_3, C_4] = \left[1, (-v), (v^2 - v)/2, (-v/6)(-v+1)(-v+2)\right], \qquad (9)$$

$$H_5 = \frac{1}{8}\begin{pmatrix} C_3 & 0 & C_3 & 0 & C_3 \\ 0 & C_2 & C_2 & C_2 & 0 \\ C_3 & C_2 & 8C_1 & C_2 & C_3 \\ 0 & C_2 & C_2 & C_2 & 0 \\ C_3 & 0 & C_3 & 0 & C_3 \end{pmatrix}, \qquad (10)$$

$$H_7 = \frac{1}{8}\begin{pmatrix} C_4 & 0 & 0 & C_4 & 0 & 0 & C_4 \\ 0 & C_3 & 0 & C_3 & 0 & C_3 & 0 \\ 0 & 0 & C_2 & C_2 & C_2 & 0 & 0 \\ C_4 & C_3 & C_2 & 8C_1 & C_2 & C_3 & C_4 \\ 0 & 0 & C_2 & C_2 & C_2 & 0 & 0 \\ 0 & C_3 & 0 & C_3 & 0 & C_3 & 0 \\ C_4 & 0 & 0 & C_4 & 0 & 0 & C_4 \end{pmatrix}, \qquad (11)$$

Adaptive behavior for various intensity levels can be implied by imparting hyperbolic profiled mapping is derived by the adaptive gain adjustment parameter (ξ) as [1]:

$$\xi = 0.5\left[1 + \tanh\left(3 - 6\left(\left|I_{fd}\right| - 0.5\right)\right)\right], \qquad (12)$$

Later on, weighted summation input intensity channel with uniformly equalized intensity channel $(\hat{I}_{en})$ can be obtained as:

$$\hat{I}_{en} = \left(\frac{\alpha}{1+\beta}\right) I_{gcp} + \left(\frac{1-\alpha}{1+\beta}\right) I_{gex} + \left(\frac{\beta}{1+\beta}\right) I_{fdmf}, \qquad (13)$$

Here, while evaluating I_{fdmf} , unfortunately over-ranging may get resulted, and it should be minimized efficiently without affecting the resulted enhancement and hence it can be included as a penalty term in the cost function framed here, as:

$$J = E.\Delta\sigma^2 . \left(\frac{\sigma^2}{\mu}\right) . \left(1 - \frac{n_{ov}}{M * N}\right), \qquad (14)$$

Here, $\mu, \sigma^2, \Delta\sigma^2$ *and* E stands for output brightness, contrast, relative contrast, and output Shannon entropy, respectively for an L-bit, $M * N$ image. Here, n_{ov} is the count of the normalized over-ranged pixels, which can be evaluated as:

$$n_{ov} = \sum\left\{\tilde{I}_{mn} < 0 \cup \tilde{I}_{mn} > 1\right\}, \qquad (15)$$

Cost-function is devised here, so that the relative variance along with maximal information restoration can be imparted with proper check on relative mean brightness. Biologically inspired and later on efficiently modified Lévy-flight Firefly Algorithm (LFA) is employed here for optimal enhancement for dark images by efficient exploration, followed by generous exploitation in a four-dimensional search space so that the required optimal values for $\alpha, \beta, v,$ and η can be obtained. The efficient parametric variation for framing search space derived analytically is $[\alpha, \beta, v, \eta] \leftarrow [(0,1), (0,5), (0.1,1), (0.1,2)]$. Following the fundamental bio-luminance based signaling behavior of fire-flies and consequently through analogous optimal idealized formulation of the flashlight; the prime objective can be resolved easily. The core idealization rules [19] when integrated with levy flight (due to its heavy-tailed probability distribution behavior) results into more efficient and highly converging approach due to significant randomization. The luminance intensity variation and consequent mutual attraction among the flies mainly decides the core efficacy of the FA; both of these issues are inter-separation distance dependent. Attractiveness (β) and luminance are highly correlated and hence minimization problem can be framed choosing relative β as a monotonically reducing expression as [19]:

$$\beta(r) = \beta_0 e^{-\tau r^m}, \qquad (m \geq 1), \qquad (16)$$

Characteristic length, $\Gamma = \tau^{-1/k} \to 1$ *as* $k \to \infty$, if τ is kept fixed and initial value can be typically taken as $\tau = \Gamma^{-m}$, considering the locations x_i, x_j for flies i, j , the spatial distance can be evaluated as [19]:

$$r_{ij} \triangleq \left\|\mathbf{x}_i - \mathbf{x}_j\right\| = \sqrt{\sum_{\delta=1}^{d}\left(x_{i,\delta} - x_{j,\delta}\right)^2}, \qquad (17)$$

Here, $x_{i,\delta}$ is the δ^{th} element of the i^{th} firefly's spatial-position $\mathbf{x}_i$. Drifting of i^{th} fly towards more attractive j^{th} fly can be characterized as [19]:

$$\mathbf{x}_i = \mathbf{x}_i + \beta_0 e^{-\tau r^2}\left(\mathbf{x}_j - \mathbf{x}_i\right) + \xi.sign\left[rand(0,1) - 0.5\right] \oplus Le'vy, \qquad (18)$$

Here, attraction and randomization (ξ) collectively constitutes the updating expression. Last term directs the randomly directed, random step size decided by $Le'vy$ distribution (with *mean and variance* $\to \infty$) as [19]:

$$Le'vy: \quad u = t^{-\lambda}, \qquad (1 < \lambda \leq 3), \qquad (19)$$

Hence, finally the above mentioned heavy tailed power-law intuitively adds the more efficient random walk process in firefly motion. Finally, optimally enhanced channel is obtained and hence, correspondingly enhanced color image can be derived as [1]:

$$\left[\hat{R}(m,n), \hat{G}(m,n), \hat{B}(m,n)\right]^T = T_{HSI}^{RGB}\left[H(m,n), S(m,n), \hat{I}(m,n)\right]^T, \qquad (20)$$

Here, T_{HSI}^{RGB} is *HSI* to *RGB* transformation process.

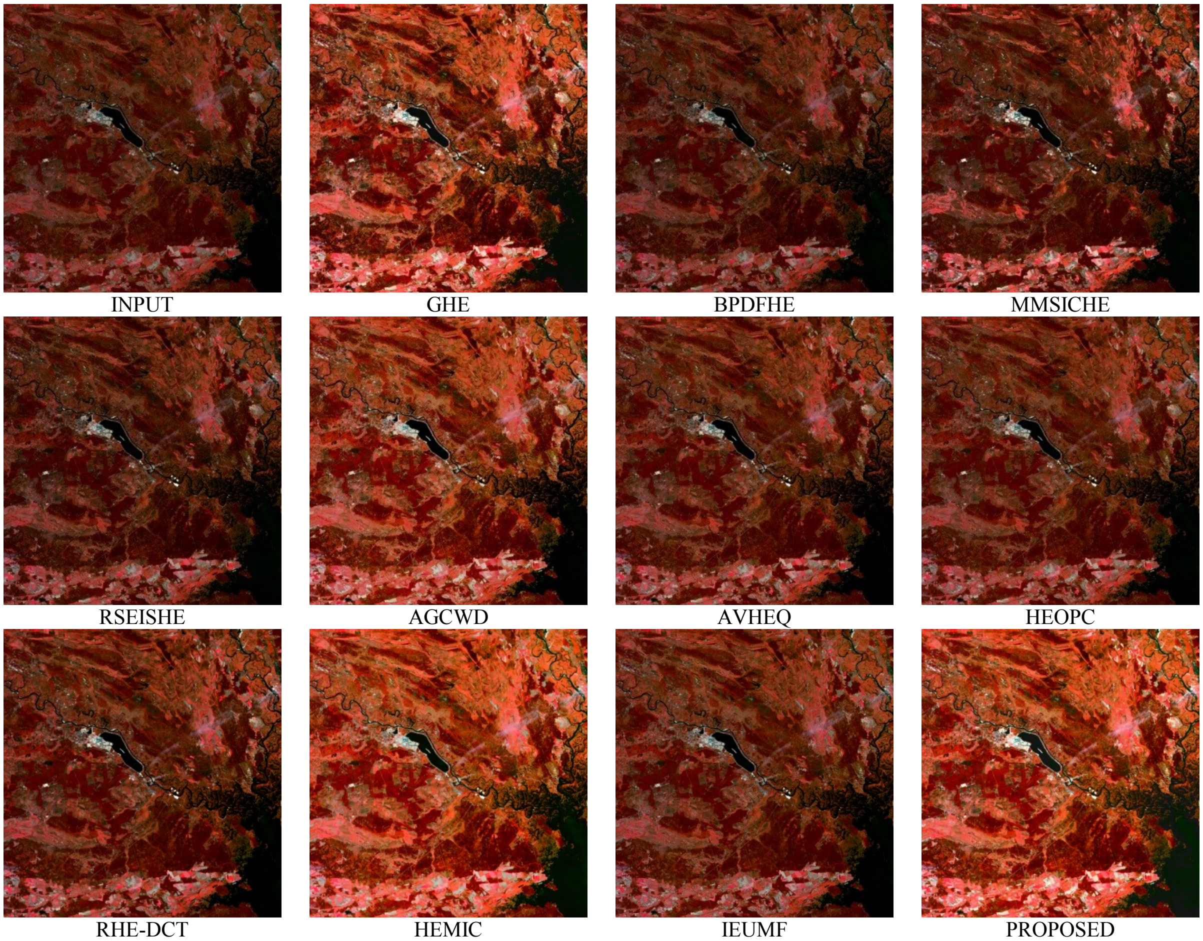

Fig. 1. Visual evaluation with comparison algorithms for "SPOT 1 Satellite Image, Chernobyl, Ukraine in 1988 [20]" among (a) input image; (b) GHE [3]; (c) BPDFHE [4]; (d) MMSICHE [5]; (e) RSEISHE [6]; (f) AGCWD [11]; (g) AVGHEQ [7]; (h) HEOPC [8]; (i) RHE-DCT [10]; (j) HEMIC [9]; (k) IEUMF [17]; and 1h-6h: the proposed approach.

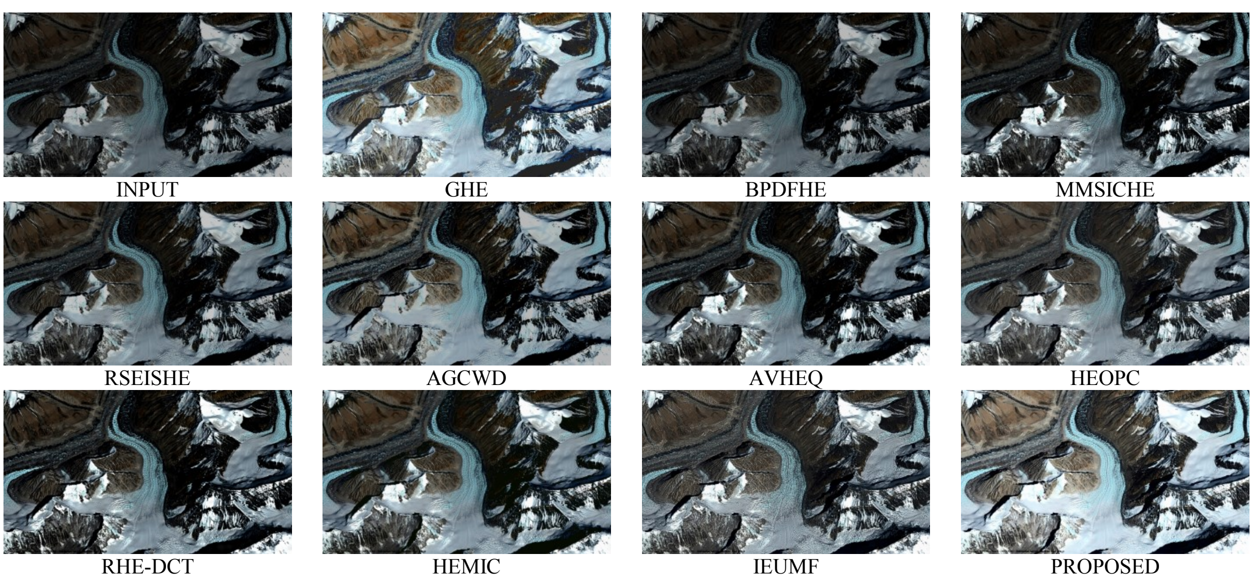

Fig. 2. Visual evaluation with comparison algorithms for "Pléiades Satellite Image – Himalayas Tibet China 2012 [20]".among (a) input image; (b) (b) GHE [3]; (c) BPDFHE [4]; (d) MMSICHE [5]; (e) RSEISHE [6]; (f) AGCWD [11]; (g) AVGHEQ [7]; (h) HEOPC [8]; (i) RHE-DCT [10]; (j) HEMIC [9]; (k) IEUMF [17]; and 1h-6h: the proposed approach.

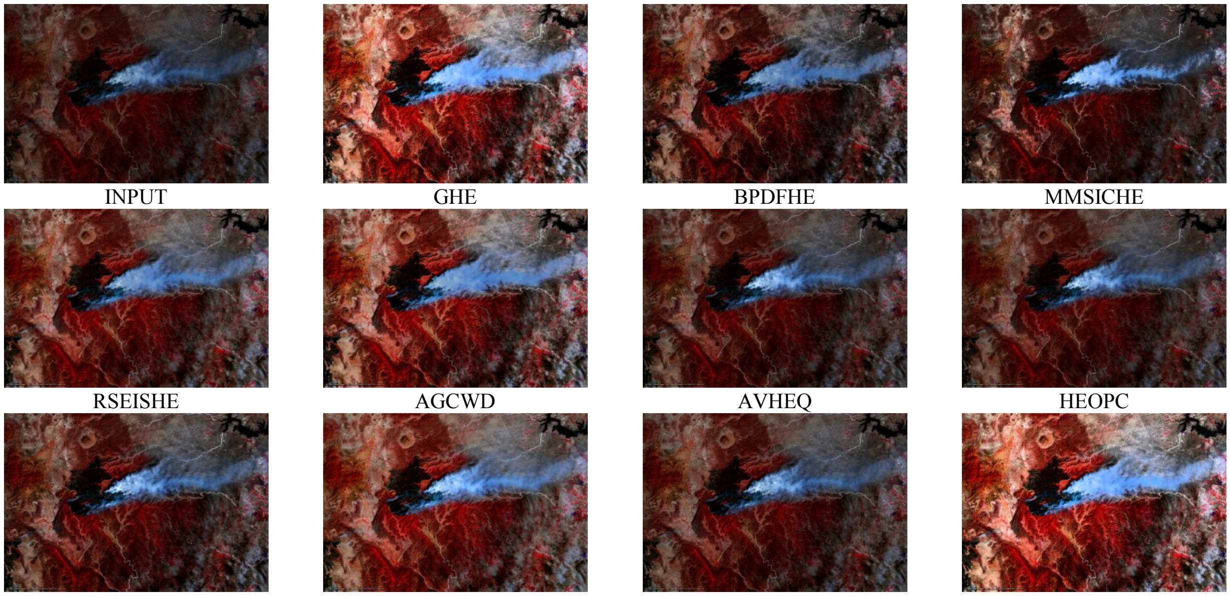

Fig. 3. Visual evaluation with comparison algorithms for "UK-DMC2 Satellite Image - Fire in Mexico [20]" among (a) input image; (b) (b) GHE [3]; (c) BPDFHE [4]; (d) MMSICHE [5]; (e) RSEISHE [6]; (f) AGCWD [11]; (g) AVGHEQ [7]; (h) HEOPC [8]; (i) RHE-DCT [10]; (j) HEMIC [9]; (k) IEUMF [17]; and 1h-6h: the proposed approach.

TABLE I

QUANTITATIVE COMPARATIVE EVALUATION AMONG INPUT IMAGES [20], GHE [3], BPDFHE [4], MMSICHE [5], RSEISHE [6], AGCWD [11], AVHEQ [7], HEOPC [8], RHE-DCT [10], HEMIC [9], IEUMF [17] AND THE PROPOSED APPROACH USING METRICS TERMED AS BRIGHTNESS (B), CONTRAST (V), ENTROPY (E), SHARPNESS (S) AND COLORFULNESS (C).

S. No.	Index	INPUT	GHE	BPDFHE	MMISCHE	RSEISHE	AGCWD	AVHEQ	HEMIC	HEOPC	HEMIC	IEUMF	OURS
1.	**B**	0.2573	0.5004	0.2955	0.2955	0.2955	0.3193	0.4243	0.3849	0.3220	0.3849	0.3237	**0.4168**
	V	0.0304	0.0859	0.0596	0.0596	0.0596	0.0492	0.063	0.052	0.0461	0.052	0.0501	**0.0779**
	E	6.8359	7.2603	7.0938	7.0938	7.0938	7.0964	7.1282	7.2701	6.9724	7.2701	7.0812	**7.3704**
	S	0.299	0.513	0.3982	0.3982	0.3982	0.3803	0.4353	0.4034	0.3694	0.4034	0.4620	**0.6087**
	C	0.1264	0.267	0.1352	0.1352	0.1352	0.156	0.2267	0.2016	0.1600	0.2016	0.1592	**0.2087**
2.	**B**	0.1265	0.5145	0.1591	0.1777	0.2819	0.3284	0.2443	0.1583	0.1653	0.314	0.1707	**0.4008**
	V	0.0139	0.0749	0.0222	0.052	0.0537	0.0687	0.047	0.0211	0.0283	0.0271	0.0323	**0.1091**
	E	5.6811	6.6078	5.8542	6.1312	6.4551	6.34	6.2811	5.8908	5.914	6.5902	5.9826	**6.4251**
	S	0.4393	1.0837	0.5616	0.7694	0.8979	1.0338	0.8304	0.5398	0.6377	0.6441	0.6833	**1.1254**
	C	0.0599	0.2559	0.0739	0.0833	0.1354	0.1601	0.1174	0.0747	0.0777	0.1686	0.0802	**0.1982**
3.	**B**	0.2235	0.4997	0.3011	0.2642	0.3577	0.4209	0.2769	0.2787	0.3062	0.41	0.2977	**0.4111**
	V	0.0146	0.0859	0.0426	0.0417	0.0332	0.0541	0.024	0.0225	0.0345	0.0399	0.0421	**0.0857**
	E	6.2797	7.0497	6.622	6.5905	6.8236	6.8929	6.5354	6.3901	6.6973	6.9547	6.7372	**7.0877**
	S	0.267	0.7052	0.4865	0.4146	0.4305	0.5596	0.343	0.3326	0.4629	0.4644	0.6867	**0.7086**
	C	0.1506	0.3465	0.2166	0.1949	0.2397	0.2877	0.1863	0.1885	0.2138	0.2773	0.2027	**0.3588**
4.	**B**	0.3519	0.5010	0.3787	0.3787	0.3787	0.6367	0.5218	0.528	0.4485	0.528	0.4671	**0.5237**
	V	0.0094	0.0859	0.0339	0.0339	0.0339	0.0544	0.0345	0.0294	0.0183	0.0294	0.0573	**0.0674**
	E	6.8800	7.2077	7.0756	7.0756	7.0756	7.6275	7.2984	7.4517	7.2257	7.4517	7.5047	**7.5311**
	S	0.2415	0.7182	0.4474	0.4474	0.4474	0.5638	0.4524	0.4254	0.3370	0.4254	0.8688	**1.0010**
	C	0.2126	0.3204	0.2288	0.2288	0.2288	0.3684	0.3169	0.3135	0.2687	0.3135	0.2950	**0.3845**
5.	**B**	0.0612	0.6079	0.1259	0.1259	0.1259	0.2692	0.1820	0.4127	0.1235	0.4127	0.1234	**0.3087**
	V	0.0071	0.0322	0.0542	0.0542	0.0542	0.1188	0.0415	0.0433	0.0281	0.0433	0.0305	**0.0602**
	E	3.0107	3.8806	3.2498	3.2498	3.2498	3.3540	3.2902	4.4715	3.8289	4.4715	3.3400	**4.6800**
	S	0.2812	0.6202	0.6980	0.6980	0.6980	1.1706	0.7130	0.6471	0.5694	0.6471	0.5945	**0.9678**
	C	0.0875	0.5103	0.2138	0.2138	0.2138	0.3768	0.2425	0.4550	0.1658	0.4550	0.1703	**0.3415**
6.	**B**	0.1446	0.5260	0.1752	0.1752	0.1752	0.1939	0.3186	0.4248	0.1811	0.4248	0.1871	**0.3919**
	V	0.0320	0.0668	0.0569	0.0569	0.0569	0.0570	0.0765	0.0501	0.0489	0.0501	0.0569	**0.0766**
	E	5.2964	6.1069	5.6815	5.6815	5.6815	5.4922	5.7146	6.3627	5.5860	6.3627	5.4880	**6.3654**
	S	0.4526	0.8683	0.5610	0.5610	0.5610	0.6203	0.9196	0.6105	0.5558	0.6105	0.6660	**0.9704**
	C	0.1228	0.3483	0.1602	0.1602	0.1602	0.1672	0.2513	0.2781	0.1521	0.2781	0.1618	**0.3701**

III. Experimentation and Result Analysis

A. Assessment Criterion

Experimentation and comparison is done qualitatively for resultant images [20] and for further quantitative assessment, performance metrics such as brightness (B), contrast/variance (V), entropy (H), sharpness (S), and colorfulness (C) for comparison among state-of the-art methods are employed, here.

B. Qualitative Assessments

For explicit analysis, reimplementation for various recent methodologies (like, GHE, BPDFHE, MMSICHE, RSEISHE, AGCWD, AVGHEQ, HEOPC, RHE-DCT, HEMIC, IEUMF) has been done. Visual results for all quality improved satellite images are presented in Fig. 1-3.

C. Quanitative Assessments

For explicit quantitative comparison and evaluation, relevant image performance metrics have been evaluated and listed in Table I.

IV. Conclusion

Concluding the outperformance of the proposed approach, it can be explicitly stated that overall quality improvement of the remotely sensed dark images can be successfully achieved through the proposed approach; along with their textural enhancement and edge content restoration. The obvious intelligence is due to application of fractionally ordered differentiation based convolutional filtering and in addition with it, counter-correction through optimally derived reciprocally dual, gamma-values. The whole weighted summation framework which itself is intuitively framed in a balanced way by using various mathematical operations in a well-organized manner including the optimal involvement of exponential, linear, convolutional-filtering and statistical operations. Nature inspired and mathematically hybridized, well-framed lévy-flight firefly algorithm (LFA) is employed for optimal solution harvesting and hence, although the proposed approach is some-how iterative, but the associated robustness and it's highly adaptive behavior counter-balances for that.

References

[1] H. Singh, A. Kumar, L. K. Balyan, and G. K. Singh, "A novel optimally weighted framework of piecewise gamma corrected fractional order masking for satellite image enhancement," *Comput. Electr. Eng.*, pp. 1–17, 2017. doi:10.1016/j.compeleceng.2017.11.014 (2017).

[2] H. Singh, A. Kumar, L. K. Balyan, and G. K. Singh, "Swarm intelligence optimized piecewise gamma corrected histogram equalization for dark image enhancement," *Comput. Electr. Eng.*, pp. 1–14, 2017. doi:10.1016/j.compeleceng.2017.06.029 (2017).

[3] R. C. Gonzalez and R. E. Woods, *Digital Image Processing*, 4th ed. Pearson/Prentice-Hall, NY, 2017.

[4] D. Sheet, H. Garud, A. Suveer, M. Mahadevappa and J. Chatterjee, "Brightness preserving dynamic fuzzy histogram equalization," *IEEE Trans. Consum. Electron.*, vol. 56, no. 4, pp. 2475-2480, Nov. 2010.

[5] K. Singh and R. Kapoor, "Image enhancement via Median-Mean Based Sub-Image-Clipped Histogram Equalization," *Optik -Int. J. Light and Electron Optics*, vol. 125, no. 17, pp. 4646-4651, Sept. 2014.

[6] K. Singh, R. Kapoor and S. K. Sinha, "Enhancement of low exposure images via recursive histogram equalization algorithms," *Optik -Int. J. Light and Electron Optics*, vol. 126, pp. 2619–2625, 2015.

[7] S. C. Huang, F. C. Cheng and Y. S. Chiu, "Efficient Contrast Enhancement Using Adaptive Gamma Correction with Weighting Distribution," *IEEE Trans. Image Process*, vol. 22, no. 3, pp. 1032-1041, Mar. 2013.

[8] S. C. F. Lin, C. Y. Wong, M. A. Rahman, G. Jiang, S . Liu, N. Kwok, H. Shi, Y.H. Yu and T. Wu, "Image enhancement using the averaging histogram equalization (AVHEQ) approach for contrast improvement and brightness Preservation," *Comput. and Elect. Eng.*, vol. 46, pp. 356-370, Aug. 2015.

[9] C. Y. Wong, G. Jiang, M. A. Rahman, S. Liu, S. C. F. Lin, N. Kwok, H. Shi, Y. H. Yu and T. Wu, "Histogram equalization and optimal profile compression based approach for colour image enhancement," *J. Visual Commun. and Image Represen.*, vol. 38, pp. 802-813, July 2016.

[10] X. Fu, J. Wang, D. Zeng, Y. Huang and X. Ding, "Remote Sensing Image Enhancement Using Regularized-Histogram Equalization and DCT," in *IEEE Geoscience and Remote Sensing Letters,* vol. 12, no. 11, pp. 2301-2305, Nov. 2015.

[11] C. Y. Wong, S. Liu, S. C. Liu, M. A. Rahman, S. C. F. Lin, G. Jiang, N. Kwok and H. Shi, "Image contrast enhancement using histogram equalization with maximum intensity coverage," *J. Modern Optics*, vol. 63, no. 16, pp. 1618-1629, Mar. 2016.

[12] H. Singh and A. Kumar, "Satellite image enhancement using beta wavelet based gamma corrected adaptive knee transformation," *IEEE Inter. Conf. on Communication and Signal Processing (ICCSP)*, Melmaruvathur, India, 2016, pp. 128-132. doi: 10.1109/ICCSP.2016.7754552

[13] H. Singh, A. Kumar, L. K. Balyan and G. K. Singh, "Dark image enhancement using optimally compressed and equalized profile based parallel gamma correction," *IEEE Int. Conf. on Communication and Signal Processing (ICCSP)*, Chennai, India, 2017, pp. 1299-1303. doi: 10.1109/ICCSP.2017.8286592

[14] H. Singh, N. Agrawal, A. Kumar, G. K. Singh and H. N. Lee, "A novel gamma correction approach using optimally clipped sub-equalization for dark image enhancement," *IEEE Int. Conf. on Digital Signal Processing (DSP)*, Beijing, China, 2016, pp. 497-501.

[15] H. Singh, A. Kumar, L. K. Balyan and G. K. Singh, "Regionally equalized and contextually clipped gamma correction approach for dark image enhancement," *IEEE Int. Conf. on Signal Processing and Integrated Networks (SPIN)*, Noida, India, 2017, pp. 431-436.

[16] H. Singh, A. Kumar, L. K. Balyan, and G. K. Singh, "A novel optimally gamma corrected intensity span maximization approach for dark image enhancement," *IEEE Int. Conf. on Digital Signal Processing (DSP)*, London, United Kingdom, 2017, pp. 1-5. doi:10.1109/ICDSP.2017.8096035.

[17] S.C.F. Lin, C.Y. Wong, G. Jiang, M.A. Rahman, T.R. Ren, N. Kwok, H. Shi, Y. H. Yu and T. Wu, "Intensity and edge based adaptive unsharp masking filter for color image enhancement," *Optik–Int. J. for Light and Electron Optics*, vol. 127, no. 1, pp. 407-414, Jan. 2016.

[18] Y.F. Pu, J. L. Zhou and X. Yuan, Fractional differential mask: a fractional differential-based approach for multiscale texture enhancement, IEEE Trans Image Process, 19 (2), 491-511, (2010).

[19] X. S. Yang, "Firefly algorithm: levy flight and global optimization,", in: Research and Development in Intelligent Systems XXVI, Springer London, pp. 209-218, 2010.

[20] Pléiades Satellite Image (https://intelligence-airbusds.com) accesed as on 01.01.2018.